Milling force measurement using a low-cost, constrained-motion dynamometer

Michael Gomez[1,2] and Tony Schmitz[1,2]
[1]Mechanical, Aerospace, and Biomedical Engineering
University of Tennessee, Knoxville
Knoxville, TN 37996, USA
[2]Energy and Transportation Science Division
Oak Ridge National Laboratory
Oak Ridge, TN 37830, USA

INTRODUCTION

The ability to measure and model cutting forces enables improved understanding of machining processes. Piezoelectric-based dynamometers currently provide the most common solution for cutting force measurement. However, the structural dynamics must be considered when operating with tooth passing frequencies near the dynamometer's multiple natural frequencies, where amplification of the local spectral content reduces accuracy. To mitigate this effect, prior research efforts have focused on two approaches. The first involves new dynamometer designs [1-9]. The second implements post-processing to remove the effect of the dynamometer's electro-mechanical "filtering" of the machining forces [10-13]. Despite these advancements, the widespread implementation of in situ cutting force measurement generally remains limited by cost and complexity.

In this paper, the design and testing of a low-cost dynamometer for milling force measurement is presented. The dynamometer design is based on constrained-motion/flexure-based kinematics. The ideally SDOF structure is excited by the cutting force to produce small amplitude displacement, which is measured using a low-cost optical interrupter (i.e., a knife edge that partially interrupts the beam in an emitter-detector pair). The force is calculated from the measured displacement using the dynamometer's FRF. This structural deconvolution is carried out by filtering the frequency domain displacement using the inverted SDOF FRF for the constrained-motion dynamometer.

STRUCTURAL DECONVOLUTION

There are five primary steps to obtaining the machining force using the constrained-motion dynamometer (CMD) [14]. These are summarized here:

1. Measure the ideally SDOF FRF for the CMD structure. In this study, the FRF was obtained using impact testing, where an instrumented hammer is used to excite the structure and the response is measured using a linear response sensor, such as a low-mass accelerometer. Ideally, the dynamometer should be mounted to the machine tool table since clamping (boundary) conditions can affect the dynamic response. Also, the test sample (to be machined) should be attached to the dynamometer because its mass affects the dynamometer's natural frequency.
2. Machine the sample using the desired axial depth of cut, radial depth of cut, feed per tooth, and spindle speed for the selected endmill-holder combination. During material removal, measure the dynamometer motion using the optical interrupter. Because the interrupter infers motion from the voltage generated by the optical detector, a calibration step is required to relate the voltage to displacement. This is typically a nonlinear relationship that can be approximated as linear over a limited displacement range (small fraction of a millimeter). In the linear case, a single calibration coefficient is used for the voltage to displacement conversion.
3. Convert the time domain displacement to the frequency domain using the discrete Fourier transform (DFT). Due to the nature of the

DFT, it is preferred to remove the transients at the cut entry and exit. The short-time Fourier transform is also an acceptable option.

4. Convert the frequency domain displacement to force using the inverted CMD FRF; see Eq. 1, where F is force, X is displacement, ω is frequency. In practice, a low pass digital filter is convolved with the inverted FRF. This is because the inverted FRF magnitude grows with increasing frequency and would otherwise amplify any high frequency noise in the displacement signal. The filter cutoff frequency is set above the dynamometer's natural frequency.
5. Once the frequency domain force is known, convert it to the time domain using the inverse DFT. The time domain force signal is then available for traditional analysis techniques, such as fitting to extract cutting force coefficients [15] or magnitude tracking to evaluate tool wear.

$$F(\omega) = [X/F\ (\omega)]^{-1} \cdot X(\omega) \quad (1)$$

DYNAMOMETER DESIGN

A monolithic, constrained-motion dynamometer was designed and constructed to measure milling forces. The design included a moving platform for workpiece mounting and four leaf-type flexure elements in an H-bar arrangement. The flexure elements guide the moving platform in the compliant direction resulting in SDOF, approximately linear motion. The emitter-detector was mounted on the base while a knife edge was attached to the moving platform (Fig. 1). The dynamometer was machined from 6061-T6 aluminium with an elastic modulus, E, of 69 GPa and a yield strength, σ_y, of 276 MPa. For the design to remain elastic, the maximum acceptable stress was selected to be $0.6\sigma_y$; as a result, the limiting stress, σ_{max}, is 160 MPa [16]. The corresponding maximum allowable displacement is:

$$\delta_{max} = \sigma_{max} \cdot L^2/3Et \approx 50\ \mu m, \quad (2)$$

where the leaf dimensions are provided in Table 1. Given δ_{max}, the dynamometer force range is ±1500 N.

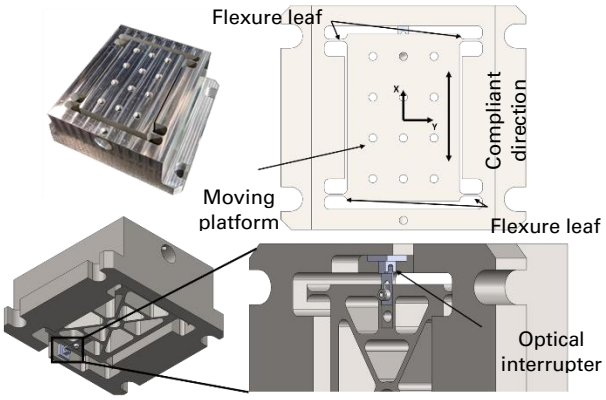

FIGURE 1. Constrained-motion dynamometer design.

TABLE 1. Flexure leaf geometry for the CMD.

Length, L (mm)	Width, b (mm)	Thickness, t (mm)
9	44.5	1.2

The optical interrupter performance was quantified using a linear air bearing positioning stage (Aerotech ABL 10100-LT). The stage had a manufacturer-specified positioning uncertainty of ±0.2 µm and resolution of 0.5 nm. The knife edge was positioned outside the emitter-detector (ROHM RPI-0352E) range and moved towards the sensor until the full range was exceeded. It was observed that the optical interrupter had a resolution of less than 1 µm with a nonlinear range of 700 µm and a linear range of 170 µm. For the linear range, the displacement sensitivity was 80 µm/V.

RESULTS

Machining trials were completed on a Haas TM-1 three-axis computer numerically controlled (CNC) milling machine. The dynamometer was mounted on the machine table with the compliant direction aligned parallel to the machine's x direction. A 6061-T6 Al workpiece (0.565 kg) was mounted on the moving platform. With this setup, x and y direction force measurement is possible with no change in dynamometer orientation. To measure x force, the feed direction is x. To measure y force, the feed direction is y. The experimental setup is detailed in Fig. 2. The cutting parameters provided in Table 2 were used for milling trials completed on both the CMD and commercial dynamometer (Kistler 9257B) for comparison.

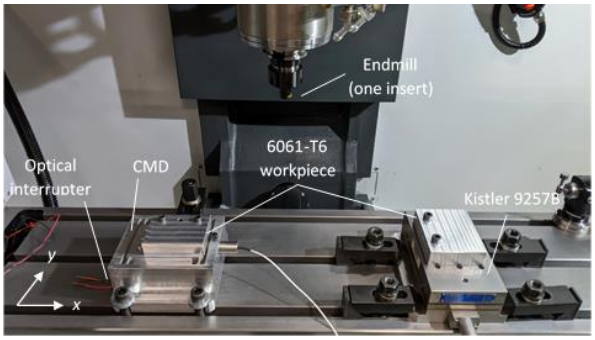

FIGURE 2. Experimental setup showing the CMD, commercial dynamometer (Kistler 9257B), endmill, and workpieces.

TABLE 2. Tool description and cutting parameters for milling trials.

Diameter (mm)	Teeth	Material
19.05	1	PVD coated micro-grain carbide
Cutting parameters for down milling tests		
Spindle speed, Ω (rpm)	1000, 2000, 3000, 4000, 5000, 6000	
Feed per tooth (mm)	0.1	
Axial depth (mm)	3	
Radial depth (mm)	1.91 (10% radial immersion)	

Impact testing results for the dynamometer are displayed in Fig. 3. For the compliant (*x*) direction, the natural frequency is 794 Hz, the stiffness is 2.6×10^7 N/m, and the viscous damping ratio is 0.0053 for the SDOF mode. Fig. 4 displays the inverse filter used to determine the force. A third-order Butterworth low pass filter (800 Hz cutoff frequency) was convolved with the inverted *x* direction FRF to avoid amplifying high frequency noise.

.

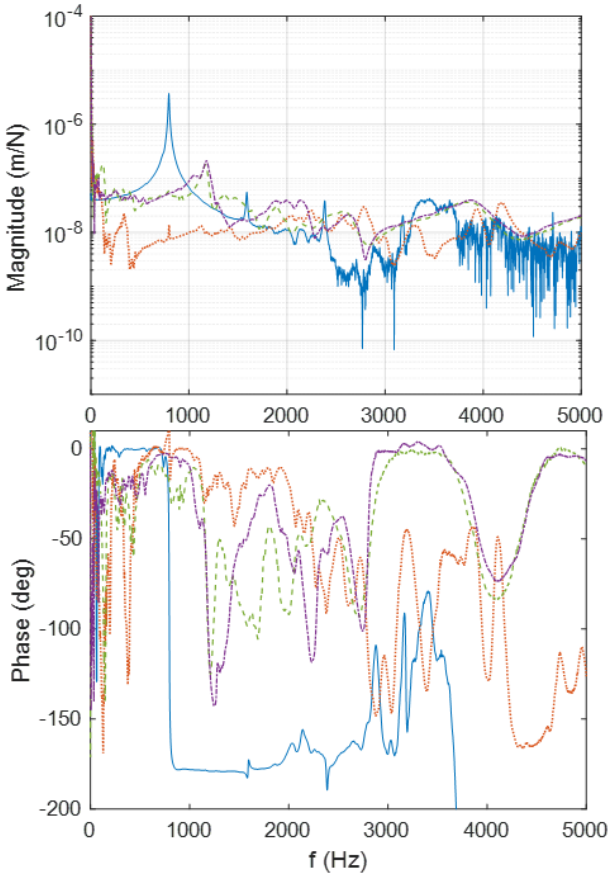

FIGURE 3. Semi-logarithmic magnitude (top) and phase (bottom) components of the CMD and tool FRFs.

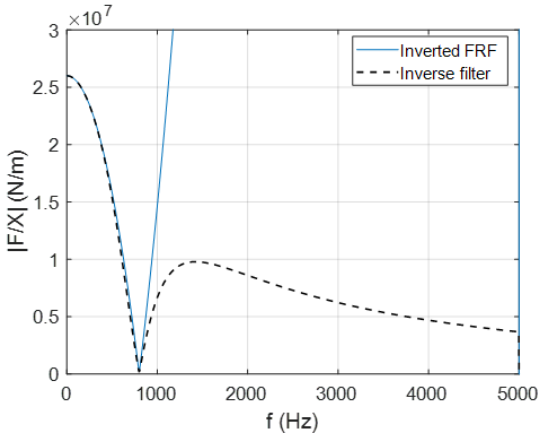

FIGURE 4. Inverted FRF and inverse filter used to determine force from measured displacement.

For each test in Table 2, the displacement was measured using the optical interrupter. Structural deconvolution was then completed to determine the force using the Fig. 4 inverse filter. Force measurements were also completed using a Kistler 9257B dynamometer for comparison. Figures 5-6 presents a comparison of the CMD

and Kistler force measurements. Good agreement is observed in Fig. 5 due to the sufficiently low spindle speed and, consequently, tooth passing frequency (16.7 Hz).

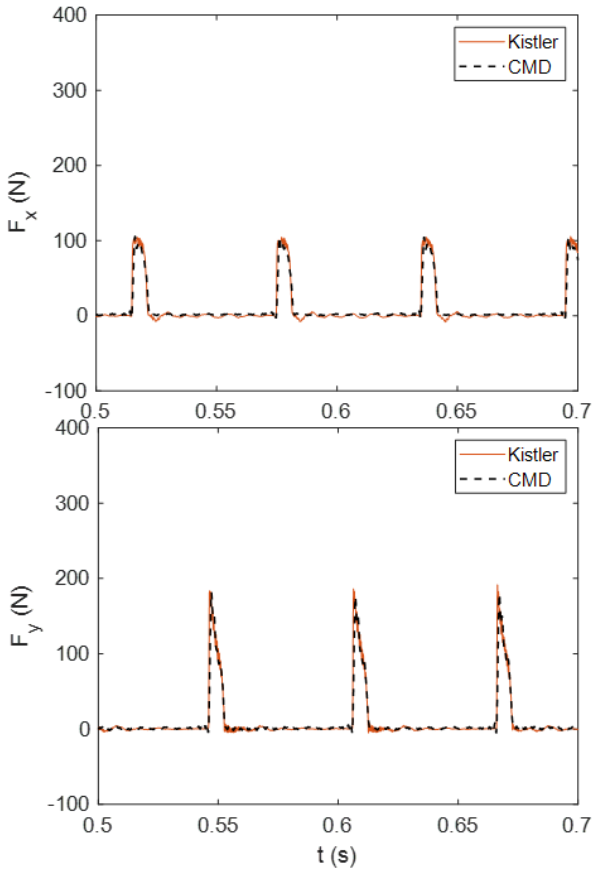

FIGURE 5. Comparison of x and y direction cutting force signals for CMD (black dashed line) and Kistler 9257B (red solid line) for a spindle speed of 1000 rpm.

At the increased spindle speed in Fig. 6 (6000 rpm, 100 Hz), however, the Kistler force because the dynamometer is itself a dynamic system and its response can be excited by the tooth passing frequency and harmonics.

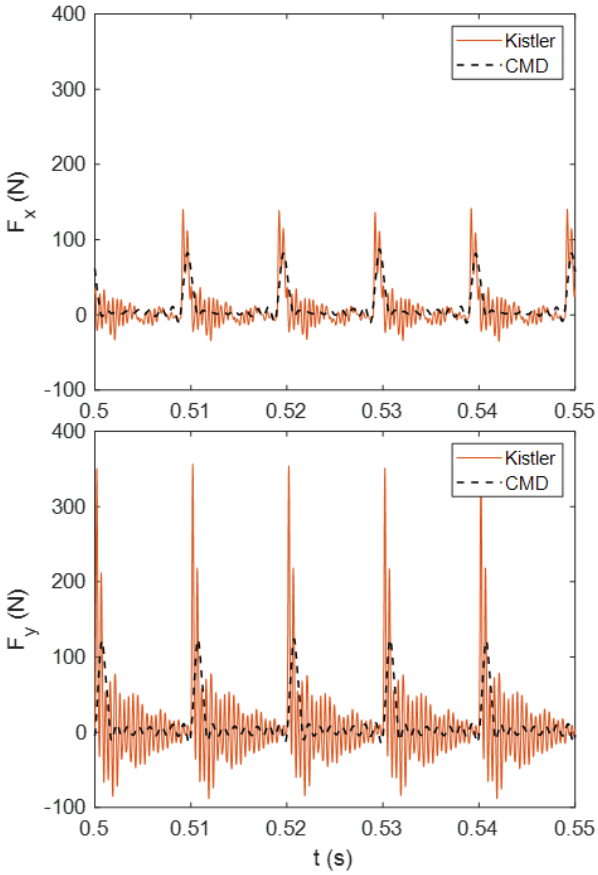

FIGURE 6. Comparison of x and y direction cutting force signals for CMD (black dashed line) and Kistler 9257B (red solid line) for a spindle speed of 6000 rpm.

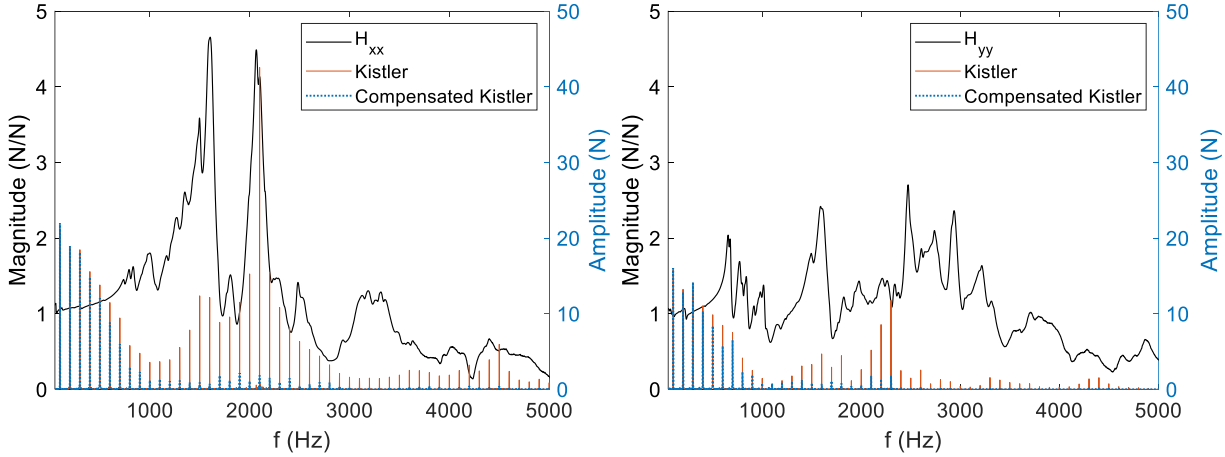

FIGURE 7. Kistler 9257B force-to-force transmissibility FRF magnitudes for the x (left) and y (right) directions (black solid line) and force frequency content: measured (red solid) and compensated (blue dashed).

The measured force-to-force transmissibility FRFs for the dynamometer's *x* (H_{xx}) and *y* (H_{yy}) directionsare shown in Fig. 7. Multiple modes are observed starting at approximately 700 Hz. The frequency content of the measured force has the expected peaks at the tooth passing frequency (100 Hz) and its harmonics. However, harmonics between 1000 Hz and 3000 Hz are artificially amplified by the dynamometer's vibration modes. To compensate for this amplification, the filtering technique described by Korkmaz et al. [12] was applied. The 1500 Hz cutoff frequency for the lowpass filter was selected such that the magnitude response of the final, inverse FRF filter is near unity at the limit of the dynamometer bandwidth, 5000 Hz. The filtered frequency content is displayed in Fig. 7, where the amplification has been effectively removed. Figure 8 demonstrates good agreement between the compensated Kistler 9257B and CMD time domain cutting force results.

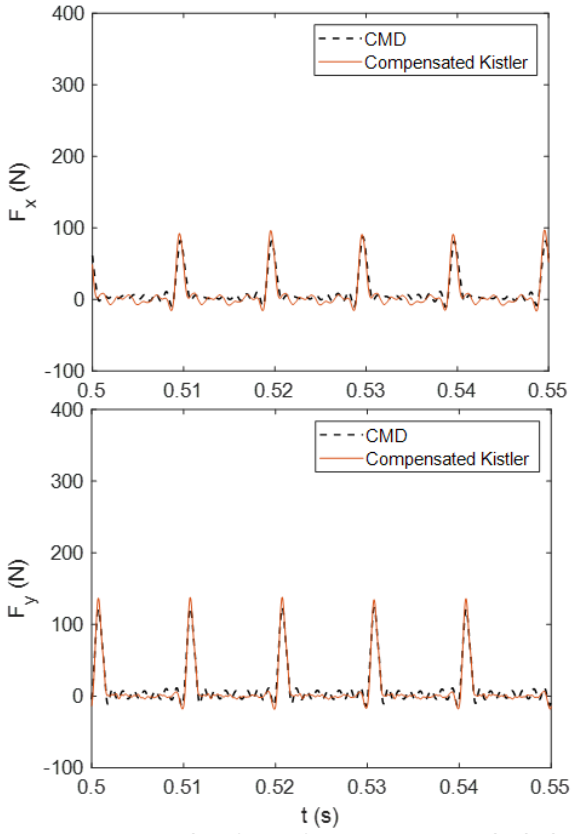

FIGURE 8. Cutting force for compensated Kistler 9257B (red solid line) and CMD (black dashed) at a spindle speed of 6000 rpm for the x and y direction forces.

To further compare the two dynamometers, the steady-state, peak values for the time domain *x* and *y* direction forces were recorded over 150 revolutions at each spindle speed. The mean values and 95% confidence intervals are presented in Fig. 9. The overlapping error bars between the CMD and compensated Kistler 9257B values demonstrate statistical agreement and validate the new low-cost CMD performance.

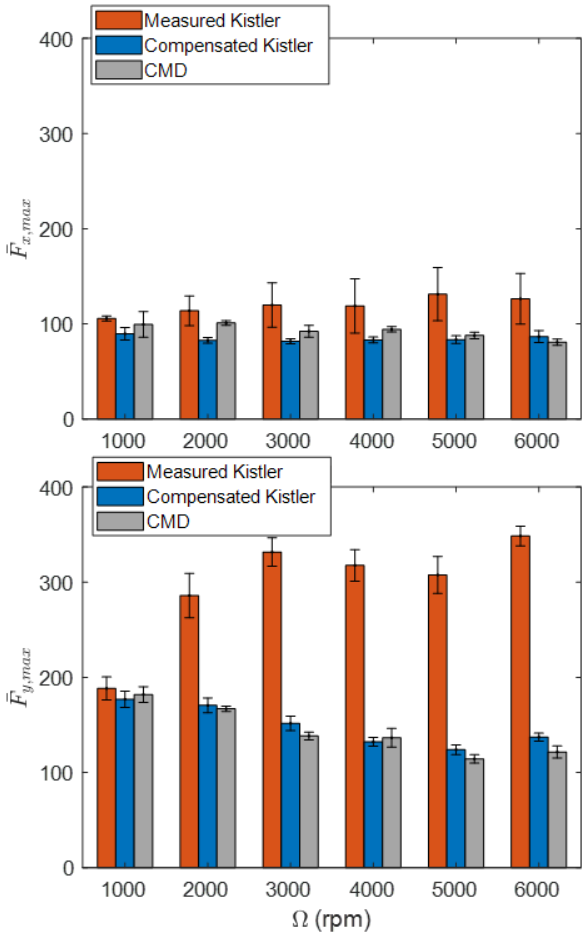

FIGURE 9. Mean peak x-direction force for the: CMD (gray), Kistler (red), and Kistler compensated (blue). Error bars indicate two standard deviations.

CONCLUSIONS

Cutting force measurement is an effective method for monitoring machining performance. The force signal can be used to optimize machine tool usage by in-process tool wear evaluation and chatter detection, for example. However, current commercially available solutions are costly and often require frequency domain signal processing to obtain accurate results.

This paper described an alternative low-cost constrained-motion dynamometer for in-process milling force measurement. The dynamometer was a monolithic design with constrained-motion of a moving platform defined by four leaf-type flexure elements arranged in the traditional H-bar configuration. An optical interrupter (fixed emitter-detector pair with a moving knife edge to partially interrupt the beam) was used to measure the moving platform's motion during milling. The cutting force was calculated from the measured displacement using the dynamometer's frequency response function (FRF). A structural deconvolution procedure was followed to filter the frequency domain displacement using the inverted dynamometer FRF and calculate the time domain force. The sensor selection, monolithic constrained-motion design, and companion structural deconvolution technique provides a low-cost, high fidelity cutting force dynamometer for use in both production and research environments.

ACKNOWLEDGEMENTS

This research was supported by the DOE Office of Energy Efficiency and Renewable Energy (EERE), Energy and Transportation Science Division and used resources at the Manufacturing Demonstration Facility, a DOE-EERE User Facility at Oak Ridge National Laboratory.

REFERENCES

[1] Santochi, M., Dini, G., Tantussi, G. and Beghini, M., 1997, A sensor-integrated tool for cutting force monitoring, CIRP Annals, 46/1: 49-52.

[2] Burton, D., Duncan, G.S., Ziegert, J., Schmitz, T., 2004, High frequency, low force dynamometer for micro-milling force measurement, Proceedings of the 19th American Society for Precision Engineering Annual Meeting, 221-224.

[3] Yaldiz, S., Unsacar, F., Haci, S., Isik, H., 2007, Design, development and testing of a four-component milling dynamometer for the measurement of cutting force and torque, Mechanical Systems and Signal Processing, 21, 1499-1511.

[4] Byrne, G. and O'Donnell, G.E., 2007, An integrated force sensor solution for process monitoring of drilling operations, CIRP Annals, 56/1: 89-92.

[5] Transchel, R. Stirnimann, J., Blattner, M., Bill, B., Thiel, R., Kuster, F., Wegener, K, 2012, Effective dynamometer for measuring high dynamic process force signals in micro machining operations, Procedia CIRP, 1, 558-562.

[6] Gu, G.M., Shin, Y.K., Son, J. and Kim, J., 2012, Design and characterization of a photo-sensor based force measurement unit (FMU), Sensors and Actuators A: Physical, 182: 49-56.

[7] Totis, G., Adams, O., Sortino, M., Veselovac, D. Klocke, F., 2014, Development of an innovative plate dynamometer for advanced milling and drilling applications, Measurement, 49, 164-181.

[8] Ettrichratz, M., Drossel, W., Gebhardt, S., Bucht, A., Kranz, B., Schneider, J., 2018, Performance of a new piezoceramic thick film sensor for measurement and control of cutting forces during milling, CIRP Annals, 67/1, 45-48.

[9] Bleicher, F., Schörghofer, P., Habersohn, C., 2018, In-process control with a sensory tool holder to avoid chatter, Journal of Machine Engineering, 18.

[10] Altintas Y., and Park S.S., 2004, Dynamic compensation of spindle-integrated force sensors, CIRP Annals, 53/1, 305-308.

[11] Castro, L.R., Vieville, P., Lipinski, P., 2006, Correction of dynamic effects on force measurements made with piezoelectric dynamometers, International Journal of Machine Tools & Manufacture, 46, 1707-1715.

[12] Korkmaz, E., Gozen, B.A., Bediz, B., Ozdoganlar, O.B., 2015, High-frequency compensation of dynamic distortions in micromachining force measurements, Procedia Manufacturing, 1, 534-545.

[13] Scippa, A., Sallese, L., Grossi, N., Campatelli, G., 2015, Improved dynamic compensation for accurate cutting force measurements in milling applications, Mechanical Systems and Signal Processing, 54-55, 314-324.

[14] Gomez, M.F., Schmitz, T., 2019, Displacement-based dynamometer for milling force measurement, Procedia Manufacturing, 34, 867-875.

[15] Rubeo, M., Schmitz, T., 2016, Mechanistic force model coefficients: A comparison of linear regression and nonlinear optimization, Precision Engineering, 45: 311-321.

[16] Smith, S.T., 2000, Flexures: Elements of Elastic Mechanisms, CRC Press, Boca Raton, FL.